

# Quantum Phase Transitions in Alternating-Bond Mixed Diamond Chains with Spins 1 and 1/2

Kazuo HIDA\*, Ken'ichi TAKANO<sup>1</sup> and Hidenori SUZUKI<sup>1†</sup>

*Division of Material Science, Graduate School of Science and Engineering,  
Saitama University, Saitama, Saitama, 338-8570, JAPAN*

<sup>1</sup>*Toyota Technological Institute, Tenpaku-ku, Nagoya 468-851, JAPAN*

(Received November 20, 2009)

We investigate the mixed diamond chain composed of spins 1 and 1/2 when the exchange interaction is alternately distorted. Depending on the strengths of frustration and distortion, this system has various ground states. Each ground state consists of an array of spin clusters separated by singlet dimers by virtue of an infinite number of local conservation laws. We determine the ground-state phase diagram by numerically analyzing each spin cluster. In particular, for strong distortions, we find an infinite series of quantum phase transitions using the cluster expansion method and conformal field theory. This leads to an infinite series of steps in the behavior of Curie constant and residual entropy.

**KEYWORDS:** mixed diamond chain, bond alternation, spin cluster, infinite series of transitions, quantum phase transition

## 1. Introduction

Frustration plays a crucial role in low-dimensional quantum magnetism.<sup>1,2)</sup> It not only drives magnetically ordered states into disordered states by enhancing quantum fluctuation but also induces magnetic moments from the disordered phase. Remarkably, there exist a class of models whose ground states are exactly written down as spin cluster states (SCSs) because of frustration. A SCS is a tensor product of exact local eigenstates of cluster spins; a dimer state is a special case.

One of the well-known examples is the Majumdar-Ghosh model, which is a spin 1/2 antiferromagnetic Heisenberg chain with next-nearest-neighbor interaction whose magnitude is half of the nearest-neighbor interaction.<sup>3)</sup> This ground state is a prototype of spontaneously dimerized phases in one-dimensional frustrated magnets. Many corresponding materials are also found as listed in ref. 4. Another well-known example is the Shastry-Sutherland model<sup>5)</sup> for which a corresponding material was synthesized 18 years after its theoretical prediction.<sup>6,7)</sup> The ground states of these models are, however, nonmagnetic. Namely, the possible magnetic (quasi-) long-range order in the unfrustrated counterpart of these models is destroyed by the enhancement of quantum fluctuation by frustration.

One of the authors and coworkers investigated a diamond chain consisting of the same kind of spin, i.e., a pure diamond chain (PDC), as an exactly treatable frustrated model.<sup>8)</sup> They found that, in the spin-1/2 case, it has two different SCSs as the ground state depending on the strength of frustration. One of them is the nonmagnetic phase accompanied by the spontaneous translational symmetry breakdown (STSB) and the other is a paramagnetic phase without STSB. It is also found that

this model has a ferrimagnetic ground state in a less frustrated region.

Modifications of the PDC have been examined by many authors. Among them, the PDC with distortion has been thoroughly investigated by numerical methods.<sup>9–11)</sup> It is found that a natural mineral azurite consists of distorted PDCs with spin 1/2. The magnetic properties of this material have been experimentally studied in detail.<sup>12,13)</sup> Other materials have also been reported.<sup>14,15)</sup> The effects of the 4-spin cyclic interaction have recently been investigated by Ivanov *et al.*<sup>16)</sup> It should be remarked that the diamond chain structure is one of the simplest structures compatible with the 4-spin cyclic interaction. The finite temperature properties of diamond chains consisting of Heisenberg bonds and Ising bonds are investigated exactly.<sup>17,18)</sup> The thermodynamic properties of a similar classical model with a hierarchical structure are also studied.<sup>19)</sup> The behavior of the residual entropy of this model is similar to that of the diamond chain.

In our previous work,<sup>20)</sup> we introduced another version of the diamond chain that consists of two kinds of spins, and named it the mixed diamond chain (MDC). Although the MDC is a simple extension of the PDC, it is a model belonging to a class different from that of the PDC in that its ground state is the Haldane state in the weak frustration region. We have investigated the MDC consisting of spins 1 and 1/2 depicted in Fig. 1(a) in special detail.<sup>20,21)</sup> Since the MDC has an infinite number of local conservation laws like the PDC, a typical ground state is a SCS consisting of spin clusters each carrying spin 1. A series of quantum phase transitions take place between five ground-state phases with different periodicities and with or without a STSB. Except in the Haldane phase, the MDC has macroscopically degenerate ground states, because each cluster has three degenerate ground states with spin 1. The SCS structures of the ground states are reflected in the characteristic thermal proper-

\*E-mail address: hida@phy.saitama-u.ac.jp

†Present address: Department of Physics, College of Humanities and Sciences, Nihon University, Setagaya-ku, Tokyo 156-8550, JAPAN

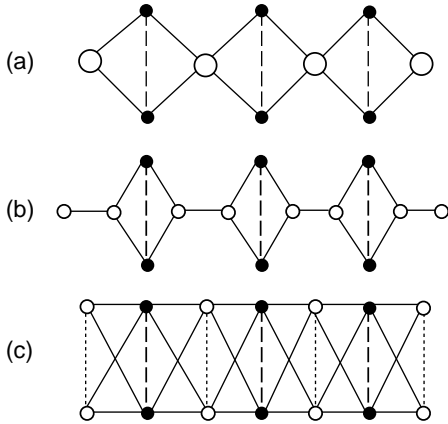


Fig. 1. Structure of (a) the mixed diamond chain and related models: (b) the dimer plaquette chain, (c) the frustrated ladder. The large open circles are spin-1 sites, The small open circles and filled circles are spin-1/2 sites.

ties, as reported in ref. 21.

The MDC is related to other important models of frustrated quantum magnetism. The dimer-plaquette model<sup>22,23</sup> shown in Fig. 1(b), which may be regarded as a one-dimensional counterpart of the Shastry-Sutherland model, reduces to the MDC if the horizontal bond in Fig. 1(b) is strongly ferromagnetic. The ground state of the dimer-plaquette model in this region has not yet been studied. In the MDC limit, however, it becomes clear that the ground state is the Haldane state. In addition, it turns out that *all* eigenstates can be expressed in terms of the eigenstates of finite-length spin 1 Heisenberg chains for an arbitrary strength of the plaquette bond in the MDC limit.<sup>20</sup>

The MDC is also related to rung-alternating frustrated Heisenberg ladders (Fig. 1(c)). If the spin 1 site in MDC is decomposed into the sum of two spin 1/2's, the MDC is equivalent to the low-energy sector of the spin 1/2 rung alternating frustrated ladder with a leg coupling equal to the diagonal coupling and one of the rung couplings is weakly antiferromagnetic or ferromagnetic. In the absence of rung alternation, it is known that this model has only Haldane and rung-dimer ground states.<sup>24</sup> However, in the MDC limit, the intermediate phases appear as explained above.

Thus far, no materials described by the MDC model have been found. Nevertheless, synthesizing MDC materials is not an unrealistic expectation in view of the success of the synthesis of many low-dimensional bimetallic magnetic compounds<sup>25</sup> and organic magnetic compounds. In the latter, spin 1 units included in a MDC material can be formed as ferromagnetic dimers.<sup>26</sup> Generally, materials with a lower symmetry have a higher chance of being found or synthesized than those with a higher symmetry. Therefore, to raise the possibility of realizing MDC materials, theoretical predictions on modified versions of the MDC model with a low symmetry are required.

The distortion is a realistic modification that lowers the symmetry of the MDC. To classify distortion patterns, we consider the normal modes of a diamond unit.

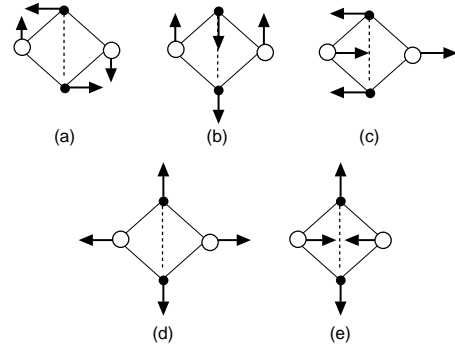


Fig. 2. Displacement modes of a diamond unit.

It has 8 degrees of freedom of displacement within the diamond plane. Excluding two translations and one rigid body rotation, we have five normal modes as depicted in Fig. 2. We may also expect that the distorted MDC can be realized as a result of the collective softening of this normal mode. Two of them ((a) and (b)) break the local conservation laws, which hold in undistorted MDCs. Among other distortion patterns ((c), (d) and (e)), (d) and (e) do not change the geometry of the original undistorted MDC. The distortion pattern (c) brings about the bond alternation in the undistorted MDC to break the original reflection symmetry. This type of distortion not only raises the possibility of the experimental realization of the MDC, but also is of theoretical importance, because in this case the eigenstates are exactly expressed as SCSs by virtue of the same local conservation laws as in the undistorted case. We hence restrict ourselves to this case in the present paper. We will show that the bond alternation distortion does not destroy the exotic phases of the undistorted MDC but even makes the ground-state phase diagram more exotic than that of the undistorted MDC. Since cases (a) and (b) contain different physics owing to effective interactions between spin clusters, they will be reported in a separate paper.

This paper is organized as follows. In §2, the model Hamiltonian is presented. In §3, the classical limit is discussed. In §4, the structure of the ground state is explained and the ground-state phases are numerically determined. In §5, an infinite series of phase transitions that occur for strong bond alternation are examined using numerical, cluster expansion, and conformal field theory methods. The last section is devoted to summary and discussion.

## 2. Hamiltonian

The alternating bond MDC is described by the Hamiltonian

$$\mathcal{H} = \sum_{l=1}^N \left\{ (1 + \delta) \mathbf{S}_l (\boldsymbol{\tau}_l^{(1)} + \boldsymbol{\tau}_l^{(2)}) + (1 - \delta) (\boldsymbol{\tau}_l^{(1)} + \boldsymbol{\tau}_l^{(2)}) \mathbf{S}_{l+1} + \lambda \boldsymbol{\tau}_l^{(1)} \boldsymbol{\tau}_l^{(2)} \right\}, \quad (1)$$

where  $\mathbf{S}_l$  and  $\boldsymbol{\tau}_l^{(\alpha)}$  ( $\alpha = 1, 2$ ) are spin 1 and spin 1/2 operators, respectively. The number of the unit cells is denoted by  $N$ . The Hamiltonian includes three types of



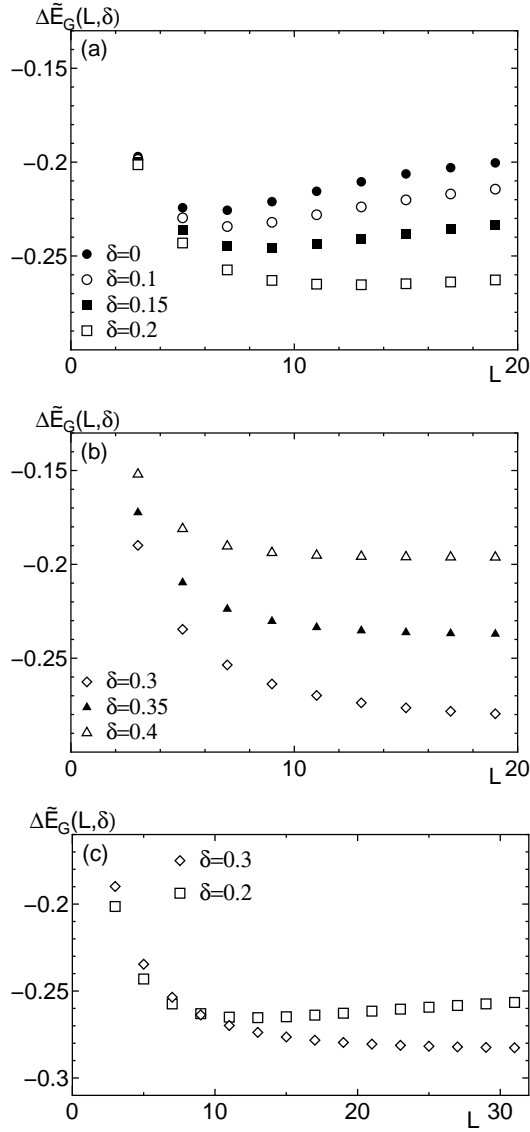


Fig. 4. Size dependence of the ground-state boundary energy  $\Delta\tilde{E}_G(L, \delta)$  of AAFH1 for (a)  $0 < \delta < \delta_c$  and (b)  $\delta > \delta_c$  obtained by numerical diagonalization, and that for (c)  $\delta = 0.2$  and  $0.3$  obtained by DMRG.

second difference of  $\tilde{E}_G(2n+1, \delta)$  with respect to  $n$ . Therefore, the  $DCn$  phase appears with a finite width as long as  $\tilde{E}_G(2n+1, \delta)$  is a convex function of  $n$ . If  $\Delta\lambda(n; \delta)$  is positive for all  $n$ , an infinite series of phase transitions take place before reaching the  $DC\infty$  phase.

We have calculated  $\tilde{E}_G(L, \delta)$  by numerical diagonalization for  $3 \leq L \leq 19$  and by the finite-size density matrix renormalization group (DMRG) for larger  $L$ . To extract the boundary contribution, we subtract the corresponding bulk energy from  $\tilde{E}_G(L, \delta)$  as

$$\Delta\tilde{E}_G(L, \delta) \equiv \tilde{E}_G(L, \delta) - (L-1)\tilde{e}_G(\infty, \delta), \quad (10)$$

where  $\tilde{e}_G(\infty, \delta)$  is the ground-state energy of the infinite-size AAFH1 per spin. This subtraction does not influence the second difference. The system size dependence of  $\Delta\tilde{E}_G(L, \delta)$  is shown in Figs. 4(a) and 4(b) for  $3 \leq L \leq 19$ . Figure 4(c) shows the data for  $L \leq 31$  for  $\delta = 0.3$  and  $0.2$ . The energy  $\tilde{e}_G(\infty, \delta)$  is estimated using the infinite-size

DMRG by measuring the bond energy of the two bonds closest to the center of the chain.

Figure 4 shows that the ground-state energy of the AAFH1 is a convex function of  $L$  for large  $\delta$  within numerical data. Therefore,  $DCn$  phases are realized for all  $n$  depending on  $\lambda$ . In contrast, for small  $\delta$ , no  $DCn$  phases with large  $n$  appear, since the ground-state energy of the AAFH1 is a concave function of  $L$  for large  $L$  as shown in Fig. 4. Actually, it is known that no  $DCn$  phases with  $n \geq 4$  appear for  $\delta = 0$ .<sup>20)</sup> In such cases, the direct transition from the  $DCn$  phase to the  $DC\infty$  phase takes place at

$$\lambda_c(n, \infty; \delta) = \tilde{E}_G(2n+1, \delta) - 2(n+1)\tilde{e}_G(\infty, \delta), \quad (11)$$

if  $\lambda_c(n, \infty; \delta) < \lambda_c(n, n+1; \delta)$ .

The phase diagram is shown in Fig. 5 using these values. At  $\delta = \delta_c \simeq 0.2598$ , where the Haldane-dimer phase transition takes place in the infinite-size AAFH1,<sup>27)</sup> the convergence of the infinite-size DMRG becomes worse. Hence, we employed extrapolation from the finite-size DMRG results to determine  $\tilde{e}_G(\infty, \delta)$ . For  $\delta < \delta_c$ , the  $DC\infty$  ground state corresponds to the uniform Haldane phase, while it corresponds to the dimer phase for  $\delta > \delta_c$ .

The phase boundary between the  $DC0$  and  $DC1$  phases is analytically obtained. Obviously,  $\tilde{E}_G(1, \delta) = 0$ , and  $\tilde{E}_G(3, \delta)$  satisfies the following eigenvalue equation within the subspace with total spin 1:

$$\tilde{E}_G(3, \delta)^3 + 4\tilde{E}_G(3, \delta)^2 + (3 - 7\delta^2)\tilde{E}_G(3, \delta) - 16\delta^2 = 0. \quad (12)$$

Therefore,  $\lambda_c(0, 1)$  satisfies

$$\lambda_c(0, 1; \delta)^3 - 4\lambda_c(0, 1; \delta)^2 + (3 - 7\delta^2)\lambda_c(0, 1; \delta) + 16\delta^2 = 0. \quad (13)$$

This relation is plotted in Fig. 5 by the thick dotted line. For  $\delta \simeq 1$ , eq. (13) implies  $\lambda_c(0, 1; \delta) \simeq 4 - 2(1 - \delta)$ .

## 5. Infinite Series of Quantum Phase Transitions

### 5.1 Almost decoupled limit: $\delta \simeq 1$

At  $\delta = 1$ , an AAFH1 with a length of  $2n+1$  is decoupled into  $n$  independent dimers and a single spin 1. Therefore, we can employ the cluster expansion method<sup>28)</sup> to estimate  $\tilde{E}_G(L, \delta)$ . The lowest-order non-vanishing contribution to  $\Delta\lambda(n; \delta)$  is  $O((1-\delta)^{2n})$  and is written as

$$\Delta\lambda(n; \delta) \simeq A_n(1+\delta) \left( \frac{1-\delta}{1+\delta} \right)^{2n} \simeq \frac{A_n}{2^{2n-1}} (1-\delta)^{2n}. \quad (14)$$

The factor  $A_n$  is given by

$$\begin{aligned} A_1 &= 4/3, \\ A_2 &= 2.305555556, \\ A_3 &= 4.501164348, \\ A_4 &= 8.794932620, \\ A_5 &= 17.01798127, \\ A_6 &= 32.60950955, \\ A_7 &= 61.96667474, \end{aligned}$$

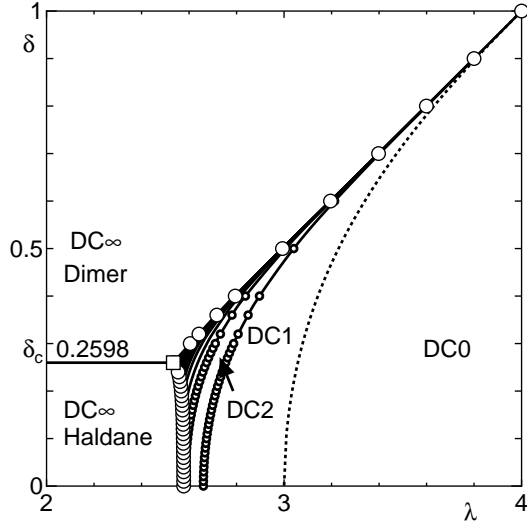


Fig. 5. Ground-state phase diagram. Small open circles are the critical points  $\lambda_c(n, n-1; \delta)$  and large open circles are the critical points  $\lambda_c(\infty, n; \delta)$ . The solid lines are guides for the eye. For  $n \geq 4$ , phase boundaries are only shown by solid lines to avoid complication. The values of  $\lambda_c(0, 1)$  calculated using eq. (13) are shown by the thick dotted line. The open square is  $\lim_{n \rightarrow \infty} \lambda_c(n, n-1; \delta_c)$ .

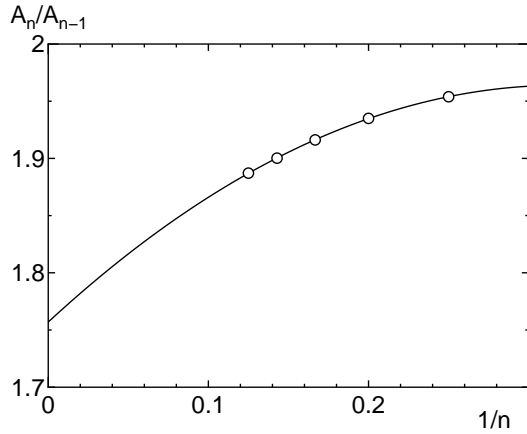


Fig. 6. Ratio  $r_n \equiv A_n/A_{n-1}$  plotted against  $1/n$ . The solid line is the least-squares fit by the second-order polynomial of  $1/n$ .

$$A_8 = 116.9402383, \quad (15)$$

up to  $n = 8$ . The ratio  $r_n \equiv A_n/A_{n-1}$  is plotted against  $1/n$  in Fig. 6. This ratio tends to converge to  $r_\infty \simeq 1.76$  and does not oscillate with  $n$ . Hence, we speculate that  $A_n > 0$  for all  $n$ . This implies that an infinite series of phase transitions take place for  $\delta \simeq 1$ .

## 5.2 $\delta = \delta_c$

Because the infinite series of phase transitions are most prominent around  $\delta = \delta_c$  in Fig. 5, we investigate this point in more detail. At this point, the ground state of the infinite AAFH1 is on the Gaussian critical point described by the conformal field theory with a conformal charge  $c = 1$ . The ground state of a cluster- $n$  is also described as a finite-size AAFH1 at the Gaussian critical point. It is known that the finite-size ground-state energy

of the Gaussian model with an open boundary condition behaves as<sup>29)</sup>

$$\tilde{E}_G(L, \delta_c) = L\tilde{\epsilon}_G(\infty, \delta_c) + \epsilon_b + \frac{A}{L}, \quad A = \frac{\pi v c}{24}, \quad (16)$$

for large  $L$ , where  $L$  is the length of the chain,  $\epsilon_b$  is the boundary energy,  $v$  is the spin wave velocity, and  $c (= 1)$  is the conformal charge.

Fitting the ground-state energy obtained using the finite-size DMRG for  $21 \leq L \leq 55$ , we obtain

$$\begin{aligned} \tilde{\epsilon}_G(\infty, \delta_c) &= -1.429085 \pm 0.000005, \\ \epsilon_b &= 1.1045 \pm 0.0005, \\ A &= 0.41 \pm 0.005, \end{aligned} \quad (17)$$

where errors are estimated by changing the smallest system size used for the fitting from 21 to 29.

Substituting eq. (16) in eq. (7), we obtain

$$\begin{aligned} \lambda_c(n-1, n; \delta_c) &= -\tilde{\epsilon}_G(\infty, \delta_c) + \epsilon_b + A \left( \frac{4n+1}{4n^2-1} \right) \\ &\simeq 2.5335 + 0.41 \left( \frac{4n+1}{4n^2-1} \right). \end{aligned} \quad (18)$$

The width of the  $DCn$  phase is given by

$$\begin{aligned} \Delta\lambda(n; \delta) &= A \left( \frac{8(n+1)}{(2n-1)(2n+1)(2n+3)} \right) \\ &\simeq 0.41 \left( \frac{8(n+1)}{(2n-1)(2n+1)(2n+3)} \right). \end{aligned} \quad (19)$$

This expression is positive for all  $n \geq 1$ . Therefore, an infinite series of phase transitions take place at  $\lambda_c(n-1, n; \delta_c)$ . It should be remarked that the width of the  $DCn$  phase decreases with  $n$  algebraically, while it decreases exponentially for  $\delta \simeq 1$  according to eq. (14). This explains why the infinite series of transitions are most visible at  $\delta = \delta_c$  in Fig. 5.

We can also estimate  $\lambda_c(n-1, \infty; \delta_c)$  as

$$\lambda_c(n-1, \infty; \delta_c) = -\tilde{\epsilon}_G(\infty, \delta_c) + \epsilon_b + \frac{A}{2n-1}, \quad (20)$$

by substituting eq. (16) in eq. (11). Thus, we obtain

$$\lambda_c(n-1, n; \delta_c) - \lambda_c(n-1, \infty; \delta_c) = \frac{2nA}{4n^2-1}. \quad (21)$$

This implies that  $\lambda_c(n-1, n; \delta_c) > \lambda_c(n-1, \infty; \delta_c)$  for all  $n \geq 1$ . This confirms our numerical conclusion that no direct transition from the  $DCn$  phase to the  $DC\infty$  phase takes place. The critical values  $\lambda_c(n-1, n; \delta_c)$  are plotted against  $n$  in Fig. 7.

## 5.3 Physical quantities

Physical quantities in the ground state is estimated in the same way as in the case of the undistorted MDC.<sup>20, 21)</sup> Because each cluster- $n$  carries a spin 1 degree of freedom, the low temperature magnetic susceptibility obeys the Curie law with the Curie constant  $C$  per unit cell given by

$$C \simeq \frac{2}{3(n+1)}, \quad (22)$$

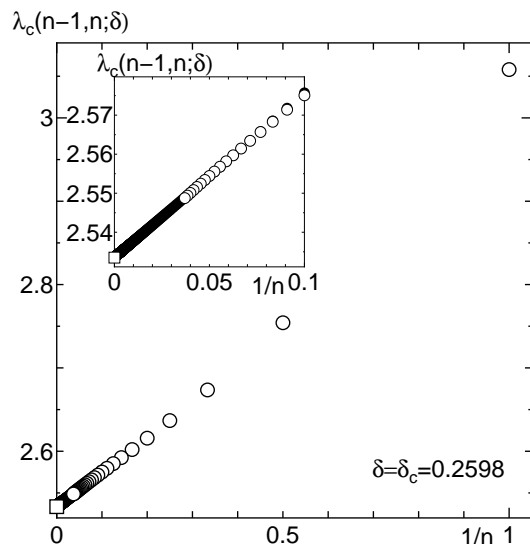


Fig. 7. Infinite series of critical points  $\lambda_c(n-1, n; \delta_c)$  at  $\delta = \delta_c$ . Open circles are calculated with eq. (7) using the values of  $\bar{E}_G(2n+1, \delta_c)$  obtained by numerical diagonalization and finite-size DMRG. Filled circles are obtained using eq. (18). The open square is  $\lim_{n \rightarrow \infty} \lambda_c(n, n-1; \delta_c)$ . The inset is an enlarged figure for large  $n$ .

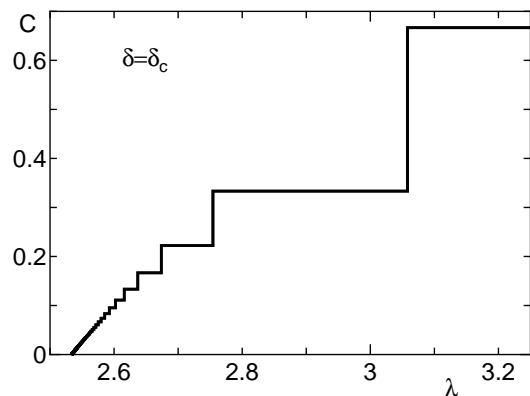


Fig. 8.  $\lambda$ -dependence of Curie constant  $C$  at  $\delta = \delta_c$ .

and the residual entropy per unit cell is given by

$$S = \frac{1}{n+1} \ln 3, \quad (23)$$

in the  $DC_n$  phase.

On the phase boundary between the  $DC(n-1)$  and  $DC_n$  phases, the residual entropy is larger than those in the  $DC_n$  and  $DC(n-1)$  phases owing to the mixing entropy of cluster- $n$ 's and cluster- $(n-1)$ 's. It is given by

$$S = -\ln \frac{1-x}{x}, \quad (24)$$

where  $x$  is the solution of

$$(n+1) \ln x - n \ln(1-x) = \ln 3. \quad (25)$$

Although these formulae (22), (23), and (24) are common to all values of  $\delta$  and  $n$  including the uniform case ( $\delta = 0$ ),<sup>20,21)</sup> the actual  $\lambda$ -dependences of these physical quantities show an infinite series of steps, if an infinite series of phase transition take place. These are plotted

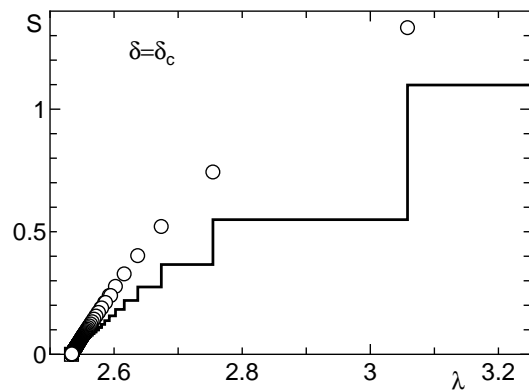


Fig. 9.  $\lambda$ -dependence of residual entropy  $S$  at  $\delta = \delta_c$ . Open circles are values on the phase boundary.

against  $\lambda$  in Figs. 8 and 9 for  $\delta = \delta_c$ , where such behavior is most clearly observed. These structures are reminiscent of the devil's staircase observed in various frustrated systems and quasiperiodic systems.<sup>30)</sup> In the case of the devil's staircase, however, physical quantities are quantized to arbitrary rational numbers and the width of the plateau decreases as the denominator increases. In contrast, in present model, the quantized values of the Curie constant and residual entropy are proportional to  $1/(n+1)$  and the numerator is fixed.

## 6. Summary and Discussion

The ground-state phases of the alternating bond MDC with spins 1 and 1/2 are investigated. Owing to the local conservation laws, the ground states are rigorously constructed, once the ground states of AAFH1s are known. Each ground-state phase is described as a  $DC_n$  phase that consists of an uniform array of cluster- $n$ 's. A cluster- $n$  is equivalent to the AAFH1 with a length of  $2n+1$ .

The ground-state phase diagram in the parameter space of the frustration  $\lambda$  and the distortion  $\delta$  is numerically determined. For  $\delta = \delta_c \simeq 0.2598$ , it is also analyzed using the conformal field theory. For  $\delta \simeq 1$ , the cluster expansion analysis is carried out. Because both analyses predict an infinite series of phase transitions with respect to  $\lambda$ , we speculate that they should take place in the entire range of  $\delta_c \leq \delta \leq 1$ . The behavior of the Curie constant and residual entropy is shown to exhibit an infinite series of steps. For small  $\lambda$ , the ground state is the  $DC_\infty$  state, which corresponds to the Haldane state for  $\delta < \delta_c$  and to the dimer state for  $\delta > \delta_c$ .

Thus, we found that the introduction of an alternating bond distortion gives rise to a rich variety of quantum phases and phase transitions in the MDC. Other types of distortion that violate the local conservation laws produce even a richer variety of phases. These will be reported in a separate paper, where the physics of the predicted phenomena are very different from the present one.

We also stress that the possibility of the experimental realization of the MDC substantially is increased by allowing the lattice distortion. We hope the experimental synthesis of the MDC and the observation of the exotic phenomena predicted in the present paper in the near

future. Variations in  $\delta$  and  $\lambda$  would be induced by the application of pressure. The infinite series of quantum phase transitions would manifest themselves as the pressure dependences of the low-temperature susceptibility and residual entropy. The substitution of nonmagnetic constituent atoms would result in similar effects. Because of the massive degeneracy in the  $DCn$  ground states, the magnetically ordered states would appear in the presence of an interchain interaction. Each ordered phase should have the periodicity of the corresponding  $DCn$  phase in the chain direction. Such a magnetic structure is observable by neutron scattering experiment.

The numerical diagonalization program is based on the package TITPACK ver.2 coded by H. Nishimori. The numerical computation in this work has been carried out using the facilities of the Supercomputer Center, Institute for Solid State Physics, University of Tokyo and the Supercomputing Division, Information Technology Center, University of Tokyo. KH is supported by a Grant-in-Aid for Scientific Research on Priority Areas, "Novel States of Matter Induced by Frustration" from the Ministry of Education, Science, Sports and Culture of Japan and by a Grant-in-Aid for Scientific Research (C) from the Japan Society for the Promotion of Science. KT and HS are supported by a Fund for Project Research from Toyota Technological Institute.

- 1) *Frustrated Spin Systems*, ed. H. T. Diep: (World Scientific, Singapore, 2005) Chaps. 5 and 6.
- 2) *Proc. Int. Conf. on Highly Frustrated Magnetism (HFM2008)* J. Phys.: Conf. Series **145** (2009).
- 3) C. K. Majumdar and D. K. Ghosh: J. Math. Phys. **10** (1969) 1399.
- 4) M. Hase, H. Kuroe, K. Ozawa, O. Suzuki, H. Kitazawa, G. Kido, and T. Sekine: Phys. Rev. B **70** (2004) 104426.
- 5) B. S. Shastry and B. Sutherland: Physica B+C **108** (1981) 1069.
- 6) H. Kageyama, K. Yoshimura, R. Stern, N. V. Mushnikov, K. Onizuka, M. Kato, K. Kosuge, C.P. Slichter, T. Goto, and Y. Ueda: Phys. Rev. Lett. **82** (1999) 3168.
- 7) H. Kageyama, M. Nishi, N. Aso, K. Onizuka, T. Yoshizawa, K. Nukui, K. Kodama, K. Kakurai, and Y. Ueda: Phys. Rev. Lett. **84** (2000) 5876.
- 8) K. Takano, K. Kubo, and H. Sakamoto: J. Phys.: Condens. Matter **8** (1996) 6405.
- 9) K. Okamoto, T. Tonegawa, Y. Takahashi, and M. Kaburagi: J. Phys.: Condens. Matter **11** (1999) 10485.
- 10) K. Okamoto, T. Tonegawa, and M. Kaburagi: J. Phys.: Condens. Matter **15** (2003) 5979.
- 11) K. Sano and K. Takano: J. Phys. Soc. Jpn. **69** (2000) 2710.
- 12) H. Kikuchi, Y. Fujii, M. Chiba, S. Mitsudo, T. Idehara, T. Tonegawa, K. Okamoto, T. Sakai, T. Kuwai, and H. Ohta: Phys. Rev. Lett. **94** (2005) 227201.
- 13) H. Ohta, S. Okubo, T. Kamikawa, T. Kunimoto, Y. Inagaki, H. Kikuchi, T. Saito, M. Azuma, and M. Takano: J. Phys. Soc. Jpn. **72** (2003) 2464.
- 14) A. Izuoka, M. Fukada, R. Kumai, M. Itakura, S. Hikami, and T. Sugawara: J. Am. Chem. Soc. **116** (1994) 2609.
- 15) D. Uematsu and M. Sato: J. Phys. Soc. Jpn. **76** (2007) 084712.
- 16) N. B. Ivanov, J. Richter, and J. Schulenburg: Phys. Rev. B **79** (2009) 104412.
- 17) L. Čanová, J. Strečka, and M. Jasčúr: J. Phys.: Condens. Matter **18** (2006) 4967.
- 18) L. Čanová, J. Strečka, and T. Lučivjanský: Condensed Matter Phys. **12** (2009) 353.
- 19) H. Kobayashi, Y. Fukumoto, and A. Oguchi: J. Phys. Soc. Jpn. **78** (2009) 074004.
- 20) K. Takano, H. Suzuki, and K. Hida: Phys. Rev. B **80** (2009) 104410.
- 21) K. Hida, K. Takano, and H. Suzuki: J. Phys. Soc. Jpn. **78** (2009) 084716.
- 22) N. B. Ivanov and J. Richter: Phys. Lett. A **232** (1997) 308.
- 23) J. Richter, N. B. Ivanov, and J. Schulenburg: J. Phys.: Condens. Matter **10** (1998) 3635.
- 24) T. Hakobyan, J. H. Hetherington, and M. Roger: Phys. Rev. B **63** (2001) 144433.
- 25) C. Mathonière, J.-P. Sutter, and J. V. Yakhmi: in *Magnetism: Molecules to Materials IV*, ed. J. S. Miller and M. Drillon: (Wiley, Weinheim, 2003) p. 1.
- 26) Y. Hosokoshi and K. Inoue: in *Carbon Based Magnetism*, ed. T. L. Makarova and F. Palacio: (Elsevier B.V., Amsterdam, 2006) p. 107.
- 27) A. Kitazawa and K. Nomura: J. Phys. Soc. Jpn. **66** (1997) 3944.
- 28) M. P. Gelfand, R. R. P. Singh, and D. A. Huse: J. Stat. Phys. **59** (1990) 1093.
- 29) H. W. Blöte, J. L. Cardy, and M. P. Nightingale: Phys. Rev. Lett. **56** (1986) 742.
- 30) P. Bak: Rep. Prog. Phys. **45** (1982) 587.